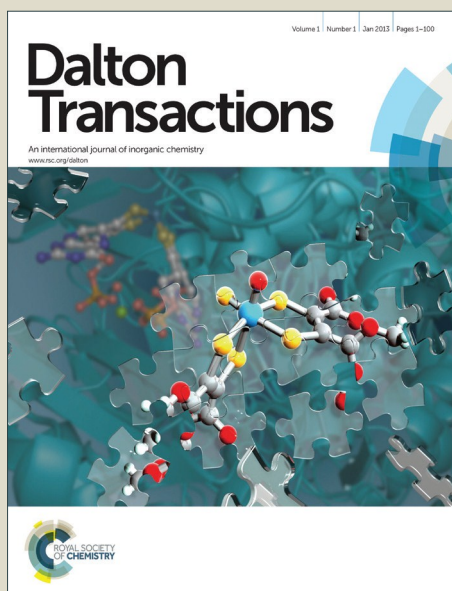


# Dalton Transactions

Accepted Manuscript



This article can be cited before page numbers have been issued, to do this please use: R. F. D'Vries, G. Gómez, J. H. Hodak, G. Soler Illia and J. A. Ellena, *Dalton Trans.*, 2015, DOI: 10.1039/C5DT04033G.



This is an *Accepted Manuscript*, which has been through the Royal Society of Chemistry peer review process and has been accepted for publication.

*Accepted Manuscripts* are published online shortly after acceptance, before technical editing, formatting and proof reading. Using this free service, authors can make their results available to the community, in citable form, before we publish the edited article. We will replace this *Accepted Manuscript* with the edited and formatted *Advance Article* as soon as it is available.

You can find more information about *Accepted Manuscripts* in the [Information for Authors](#).

Please note that technical editing may introduce minor changes to the text and/or graphics, which may alter content. The journal's standard [Terms & Conditions](#) and the [Ethical guidelines](#) still apply. In no event shall the Royal Society of Chemistry be held responsible for any errors or omissions in this *Accepted Manuscript* or any consequences arising from the use of any information it contains.



Journal Name

ARTICLE

## Tuning the Structure, dimensionality and Luminescent properties of Lanthanide Metal-Organic Frameworks under Ancillary Ligand Influence. †

Richard F. D'Vries,<sup>a\*</sup> German E. Gomez,<sup>b</sup> José H. Hodak,<sup>c</sup> Galo J. A. A. Soler-Illia,<sup>b</sup> Javier Ellena.<sup>a</sup>Received 00th January 20xx,  
Accepted 00th January 20xx

DOI: 10.1039/x0xx00000x

www.rsc.org/

This manuscript addresses the synthesis, structural characterization and optical properties of a 1D coordination polymer (CPs) and 2D and 3D Metal-Organic Frameworks (MOFs) obtained from lanthanide metals, 3-Hydroxynaphthalene-2,7-disulfonic acid (3-OHNDS) and two different phenanthroline derivatives as ancillary ligands. The first is a family of 2D compounds with formula  $[\text{Ln}(\text{3-OHNDS})(\text{H}_2\text{O})_2]$ , where Ln = La(1), Pr(2), Nd(3) and Sm(4). The addition of 1,10-phenanthroline (phen) in the reaction produces 1D compounds with general formula  $[\text{Ln}(\text{3-OHNDS})(\text{phen})(\text{H}_2\text{O})]\cdot 3\text{H}_2\text{O}$ , where Ln = La(5), Pr(6), Nd(7) and Sm(8). Finally, the synthesis with 3,4,7,8-tetramethyl-1,10-phenanthroline (3,4,7,8-TMPhen) as an ancillary ligand results in the formation of the 3D  $[\text{La}(\text{3-OHNDS})(\text{3,4,7,8-TMphen})(\text{H}_2\text{O})]$  (9) compound. The photoluminescence (PL) properties of 1D and 2D compounds were fully investigated in comparison with the 3-OHNDS ligand. One of the most important results was the obtention of a white-light single-emitter without adding dopant atoms in the structure. With all these results in mind was possible establish structure-properties relationships.

### Introduction

Over the past two decades, coordination polymers (CPs) and metal-organic frameworks (MOFs) have been widely studied. Many types of MOFs are designed from diverse metallic centers and ligands and by different methodologies.<sup>1</sup> For instance, using small aliphatic linkers as oxalate and succinate was possible synthesized MOFs with interesting optical and catalytic properties.<sup>2-5</sup> On the other hand, the use of large multitopic aromatic molecules results in structures with large cavities used in gas absorption.<sup>6-8</sup> Peng, *et al.* reported the use of "macromolecules" as functionalized fullerenes in the formation 2D fullerene-linked structures<sup>9</sup> and more recently Sontz *et al.* constructed a MOF using spherical protein as nodes.<sup>10</sup> All these new compounds are synthesized for the obtaining of new crystalline materials with high internal surface areas to be used for gas storage,<sup>11, 12</sup> chemical separation,<sup>13, 14</sup> chemical sensing,<sup>15, 16</sup> drug delivery<sup>17, 18</sup> or as

heterogeneous catalysts.<sup>19-21</sup> Besides these properties associated with internal voids in the MOFs, physical-chemical properties, as luminescence,<sup>16, 22-25</sup> magnetism<sup>26</sup> and conductivity<sup>27, 28</sup> are part of the multiple applications of these versatile and promising materials.

Moreover, lanthanide-metal organic frameworks (Ln-MOFs) have drawn increasing interest because of their fascinating topological structures and fantastic photoluminescence (PL) properties.<sup>29</sup> However, it is well-known that Ln<sup>III</sup> metallic centers cannot efficiently absorb light due to forbidden *4f-4f* transitions (extinction coefficients are approximately 1-10 M<sup>-1</sup> cm<sup>-1</sup>).<sup>25</sup> A strategy for the sensitization of Ln-MOFs is to incorporate chromophores either as ligands, or a guest molecules acting as antennas for light absorption and then transfer the energy to the emitter centers (antenna effect).<sup>30</sup> Numerous works reports the use of chromophoric antenna ligands, in particular,  $\pi$ -conjugated organic molecules in the synthesis of photoluminescent materials.<sup>31</sup>

Inside multitopic molecules used as linkers disulfonaphthalene is part of a family of ligands that can be used as rigid pillars in the formation of compounds of high thermal stability, porosity, good crystallization ability and whose structures present different dimensionalities, architectures, topologies and/or supramolecular structures.<sup>32-35</sup> Previous reports have addressed the weak coordination character of sulfonate groups,<sup>36, 37</sup> however, an extensive study along the past years has shown aryl-sulfonate molecules used as linkers in the formation of MOFs have high coordination ability in the presence of lanthanide metals and ancillary ligands, under solvothermal reaction conditions.

<sup>a</sup> Instituto de Física de São Carlos, Universidade de São Paulo, CEP. 13566-590, São Carlos - SP, Brasil.

<sup>b</sup> Gerencia de Investigación y Aplicaciones, Centro Atómico Constituyentes, Comisión Nacional de Energía Atómica, Grupo de Nanoquímica Av. Gral. Paz 1499, 1650 San Martín, Buenos Aires, Argentina.

<sup>c</sup> DQIAYQF and INQUIMAE-CONICET FCEN Universidad de Buenos Aires, Pab. II Ciudad Universitaria CABA1428, Buenos Aires Argentina.

†Electronic Supplementary Information (ESI) available: [Experimental X-ray powder patterns, TG analysis, IR spectra, excitation spectrum, assignment of the transitions in the excitation and emission spectra, Luminescence decay traces and CIE coordinates and color emission for  $[\text{Ln}(\text{3-OHNDS})(\text{H}_2\text{O})_2]$ ,  $[\text{Ln}(\text{3-OHNDS})(\text{phen})(\text{H}_2\text{O})]\cdot 3\text{H}_2\text{O}$  and  $[\text{La}(\text{3-OHNDS})(\text{3,4,7,8-TMphen})(\text{H}_2\text{O})]$  compounds. CCDC reference numbers 1422484-1422487 and 1426613-1426617 contains the supplementary crystallographic data for this paper]. See DOI: 10.1039/x0xx00000x

## ARTICLE

## Journal Name

On the another hand, the use of phenanthrolines as ancillary ligands can produce compounds that not only increase the rigidity of MOF structures, but also provide a powerful absorbing sensitizer. Moreover, a certain degree of rigidity and robustness of phenanthroline moiety are also helpful for keeping the coordination sphere and reducing the non-radiative deactivation.<sup>38</sup>

This manuscript addresses the synthesis of nine new compounds from 3-hydroxinaftalene-2,7-disulfonic acid (3-OHNDS), the first metals of the lanthanide series and two different phenanthroline derivatives as ancillary ligands. They were thermally and spectroscopically characterized and the covalent and supramolecular networks were analyzed so that their topology could be found. In addition, a complete photoluminescence properties study was realized in order to test the sensitization ability of 3-OHNDS and in combination with the ancillary ligands.

## Experimental Section

### General information.

All reagents and solvents employed were commercially available and used as supplied with no further purification: 3-Hydroxinaftalene-2,7-disulfonic acid (95%, Sigma-Aldrich); 1,10-phenanthroline (99 %, Sigma-Aldrich); 3,4,7,8-tetramethyl-1,10-phenanthroline (99 %, Sigma-Aldrich); Ln(NO<sub>3</sub>)<sub>3</sub>·6H<sub>2</sub>O where Ln = La, Pr, Nd, Sm, Eu, Gd, Tb and Ho (99%, Sigma-Aldrich). Powder X-ray diffraction (PXRD) patterns were measured with a Rigaku Ultima IV diffractometer of 0.02° step size and 2 s/step exposure time. PXRD measurements proved the isostructurality of the series and the purity of the obtained microcrystalline products by the comparison of the experimental results with the simulated pattern obtained from single crystal X-ray diffraction data. IR spectra were recorded from KBr pellets in the 4000-250 cm<sup>-1</sup> range on a Bomem Michelson FT MB-102. Thermogravimetric analyses (TGA) were performed in Shimadzu TGA-50 equipment at 25-900 °C temperature range, under nitrogen (100 mL/min flow) atmosphere and 10 °C/min heating rate. A Fisons EA-1108 CHNS-O was employed for the elemental analysis.

### Synthesis.

Several temperatures and reaction times were tested. The molar composition of the initial reaction mixture in 3-OHNDS<sup>3</sup>:Ln<sup>3+</sup>:1474H<sub>2</sub>O and two equivalents for the ancillary ligands were set. The optimized synthesis procedure is described as follows:

**[La(3-OHNDS)(H<sub>2</sub>O)<sub>2</sub>]** was obtained by the addition of 3-OHNDS (0.04 g, 0.115 mmol) to a solution of La(NO<sub>3</sub>)<sub>3</sub>·6H<sub>2</sub>O (0.05 g, 0.115 mmol) in 6 mL of water. The reaction mixture was adjusted to pH≈6 by the addition of NaOH 1M, under constant stirring at room temperature for 30 minutes. Finally, the reaction mixture was placed in a Teflon-lined stainless steel autoclave for reacting under hydrothermal conditions at 170°C for 18 hours. After cooling to room temperature, the crystalline products were filtered and washed with water and ethanol and a yield of 40.1 % was obtained. The same procedure was conducted for the synthesis of **[Ln(3-**

**OHNDS)(H<sub>2</sub>O)<sub>2</sub>]**, where Ln = La(1), Pr(2), Nd(3) and Sm(4). Elemental analysis calculated for **[La(3-OHNDS)(H<sub>2</sub>O)<sub>2</sub>]**: C, 25.12; H, 1.90; S,13.41; found: C, 24.85 ; H,2.3; S, 12.86 .

**[La(3-OHNDS)(phen)(H<sub>2</sub>O)]·3H<sub>2</sub>O** was obtained by the addition of 3-OHNDS (0.04 g, 0.115 mmol) and 1,10-phenanthroline (0.06 g, 0.33 mmol) to a solution of La(NO<sub>3</sub>)<sub>3</sub>·6H<sub>2</sub>O (0.05 g, 0.115 mmol) in 6 mL of water. The reaction mixture was stirred at room temperature for 30 minutes and placed in a Teflon-lined stainless steel autoclave for reacting under hydrothermal conditions at 180°C for 20 hours. After cooling to room temperature, the crystalline products were filtered and washed with water and ethanol and a yield of 68.2 % was obtained. The same procedure was employed for the synthesis of **[La(3-OHNDS)(phen)(H<sub>2</sub>O)]·3H<sub>2</sub>O**, where Ln = La(5), Pr(6), Nd(7) and Sm(8). Elemental analysis calculated for **[La(3-OHNDS)(phen)(H<sub>2</sub>O)]·3H<sub>2</sub>O**: C, 38.16; H, 3.6; N, 4.05; S,9.26; found: C, 38.65; H, 3.10; N, 4.14; S, 8.41.

**[La(3-OHNDS)(3,4,7,8-TMphen)(H<sub>2</sub>O)]** (9) was obtained by the addition of 3-OHNDS (0.024 g, 0.07 mmol) and 3,4,7,8-tetramethyl-1,10-phenanthroline (0.033 g, 0.14 mmol) to a solution of La(NO<sub>3</sub>)<sub>3</sub>·6H<sub>2</sub>O (0.03 g, 0.07 mmol) in 6 mL of water. The reaction mixture was stirred at room temperature for 30 minutes and placed in a Teflon-lined stainless steel autoclave for reacting under hydrothermal conditions at 170°C for 17 hours. After cooling to room temperature, the crystalline products were filtered and washed with water and ethanol and a yield of 55.6 % was obtained. Elemental analysis calculated for **[La(3-OHNDS)(3,4,7,8-TMphen)(H<sub>2</sub>O)]**: C, 44.96; H, 3.34;N, 4.03 S,9.23; found: C,44.39; H,4.07; N, 3.99; S, 8.52.

### Single-Crystal structure determination.

Single-crystal X-ray data for compounds (1)-(7) and (9) were collected at room temperature (298 K) on an Enraf-Nonius Kappa-CCD diffractometer using MoK $\alpha$  radiation (0.71073 Å) monochromated by graphite. The cells were refined by Collect and Scalepack software and their final parameters were obtained on all reflections. A data reduction was carried out by Denzo-SMN and Scalepack software.<sup>39</sup> The compound (8) was collected on an Bruker APEX-II CCD diffractometer using MoK $\alpha$  radiation (0.71073 Å) monochromated by graphite. The cell determination and the final cell parameters were obtained on all reflections using the software Bruker SAINT included in APEX2 software suite.<sup>40</sup> Data integration and scaled was carried out using the software Bruker SAINT.<sup>41</sup> The structures were solved by SHELXS-2013 software and then refined by SHELXL-2013,<sup>42</sup> included in WinGX<sup>43</sup> and Olex2.<sup>44</sup> Non-hydrogen atoms of the molecules were clearly resolved and their full-matrix least-squares refinement with anisotropic thermal parameters was conducted. All hydrogen atoms were stereochemically positioned and refined by the riding model.<sup>42</sup> Hydrogen atoms of the water molecules were localized and fixed (with Uiso(H) = 1.5Ueq) on the density map. ORTEP diagrams were prepared with Diamond.<sup>45</sup> TOPOS,<sup>46</sup> Mercury<sup>47</sup> and Diamond<sup>45</sup> programs were used in the preparation of the artwork of the polyhedral and topological representations. A disordered solvent molecule was identified in the final stages

of refinement for the compounds (1)-(4) and (9). This highly disordered region of the asymmetric unit was treated by application of the program Squeeze as implemented in Platon<sup>48</sup> which allows for the mathematical compensation of the electron contribution of disordered solvent contained in the voids to the calculated diffraction intensities. The results of the Squeeze treatment are shown in the Table S3 (Supp. Inf. S8).

#### X-ray powder diffraction.

(PXRD) patterns were measured with a Rigaku Ultima IV diffractometer of 0.02° step size and 2 s/step exposure time. The measurements were used to prove the isostructurality of the series and check the purity of the microcrystalline products obtained by the comparison of the experimental results with the simulated pattern provided by single crystal X-ray diffraction data.

#### Photoluminescence (PL) measurements.

The PL measurements were taken on a Félix X32 PTI fluorometer setup equipped with a UXL-75Xe xenon short-arc lamp. The excitation-emission spectra of the free 3-OHNS ligand and compounds (1)-(8) were measured in N,N-dimethylformamide ( $\geq 99.8\%$ , Biopack) suspensions (10 milligrams of the compound in 3 mL of DMF). Prior to the PL studies, the closed glass vials containing the samples were ultrasonicated at 80 KHz (in a Cleanson apparatus) for 30 minutes for the obtaining of homogeneous suspensions. The slit widths for excitation and emission were 1.5. Luminescence spectra were recorded at room temperature between 350-550 nm for 3-OHNS, 400-500 nm for (1) and (5), 430-750 nm for (2), (4), (6) and (8), and 350-600 nm for compounds (3) and (7), all with identical operating conditions and the lamp on to ensure a valid comparison between the emission spectra. The data were collected at every nanometer with an integration time of 0.1 seconds for each step. The (x,y) Commission Internationale de l'Eclairage (CIE) color coordinates were calculated by MATLAB® program with .txt data emission as input files. Time resolved luminescence measurements were carried out using the output of a femtosecond optical parametric amplifier with excitation at 350nm (<200 fs FWHM pulses) (Coherent Legend and OperaSolo). The emission was collected at right angle from excitation, with a 2.5 cm focal length lens and focused on the entrance of a monochromator (Oriel 77250) with a second 2.5 cm focal length lens. A 390nm interference cut-off filter was used to further reject scattered light at 350nm. The signal was detected with a photomultiplier tube (Hamamatsu R928) operated at 700V and a 500 MHz digitizing oscilloscope (Agilent MSO5062A).

## Results and discussion.

#### Structural description of Ln- MOFs.

Details of data collection, refinement and crystallographic data for the compounds are summarized in Table 1. The ORTEP

diagrams for [Ln(3-OHNS)(H<sub>2</sub>O)<sub>2</sub>], [Ln(3-OHNS)(phen)(H<sub>2</sub>O)]·3H<sub>2</sub>O (where Ln = La, Pr, Nd and Sm) and [La(3-OHNS)(3,4,7,8-TMphen)(H<sub>2</sub>O)] compounds are shown in Fig. 1.

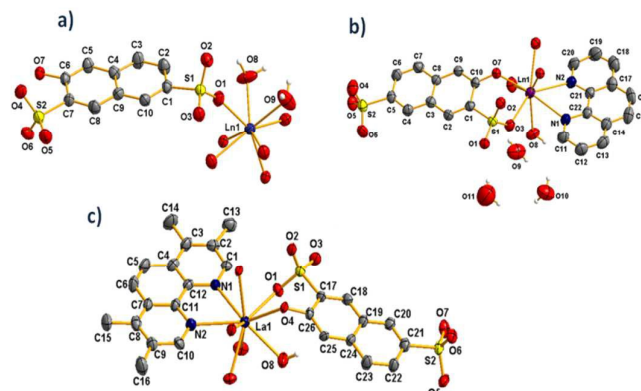


Fig. 1 ORTEP diagram showing 50% of probability ellipsoids [Ln(3-OHNS)(H<sub>2</sub>O)<sub>2</sub>], [Ln(3-OHNS)(phen)(H<sub>2</sub>O)]·3H<sub>2</sub>O (where Ln = La, Pr, Nd and Sm) and [La(3-OHNS)(3,4,7,8-TMphen)(H<sub>2</sub>O)] compounds. Hydrogen atoms were removed for clarity.

Table 1 Crystallographic data and refinement parameters for [Ln(3-OHNS)(H<sub>2</sub>O)<sub>2</sub>], [Ln(3-OHNS)(phen)(H<sub>2</sub>O)]·3H<sub>2</sub>O and [La(3-OHNS)(3,4,7,8-TMphen)(H<sub>2</sub>O)] compounds.

Compound	(1)	(2)	(3)	(4)
Emp. Formula	C <sub>10</sub> H <sub>9</sub> O <sub>9</sub> S <sub>2</sub> LaC <sub>10</sub>	H <sub>9</sub> O <sub>9</sub> S <sub>2</sub> PrC <sub>10</sub>	H <sub>9</sub> O <sub>9</sub> S <sub>2</sub> NdC <sub>10</sub>	H <sub>9</sub> O <sub>9</sub> S <sub>2</sub> SmC <sub>10</sub>
FW (g/mol)	476.21	478.21	481.54	487.67
Temp. (K)	293	293	293	293
λ (Å)	0.71073	0.71073	0.71073	0.71073
Crystal system	Monoclinic	Monoclinic	Monoclinic	Monoclinic
Space Group	C2/c	C2/c	C2/c	C2/c
Unit cell				
a (Å)	17.6665(5)	17.5597(6)	17.5398(6)	17.5594(7)
b (Å)	22.7226(6)	22.6337(7)	22.5802(7)	22.4319(9)
c (Å)	8.5749(3)	8.5253(3)	8.5187(3)	8.4604(2)
β (°)	118.320(1)	118.362(2)	118.427(2)	118.585(2)
Volume (Å <sup>3</sup> )	3030.22(16)	2981.59(18)	2967.05(18)	2926.27(19)
z	8	8	8	8
ρ calcd (mg/m <sup>3</sup> )	2.087	2.131	2.156	2.214
Abs.Coeff (mm <sup>-1</sup> )	3.136	3.589	3.825	4.341
F(000)	1839	1856	1864	1880
θ range (°)	3.0 to 26.3	3.0 to 26.3	3.0 to 26.3	3.0 to 26.4
Reflections collected / Unique [R(int)]	6036 / [0.036]	24493 / [0.106]	21329 / [0.089]	24647 / [0.110]
Completeness (%)	99.7	99.9	99.6	99.7
Data / restraints / parameters	3080/0/206	3041/0/206	3010/0/205	3002/0/201
Gof on F <sup>2</sup>	0.95	0.95	0.93	0.94
R1 [I>2σ(I)]	0.0433	0.0473	0.0461	0.0419
wR2 [I>2σ(I)]	0.1071	0.1168	0.1152	0.0993

Compound	(5)	(6)	(7)	(8)	(9)
	$C_{22}H_{15}N_2O_8S_2La$	$C_{22}H_{15}N_2O_8S_2Pr$	$C_{22}H_{15}N_2O_8S_2Nd$	$C_{22}H_{15}N_2O_8S_2Sm$	$C_{52}H_{46}La_2N_4O_{19}$
Emp. Formula	3(H <sub>2</sub> O)	3(H <sub>2</sub> O)	3(H <sub>2</sub> O)	3(H <sub>2</sub> O)	S <sub>4</sub>
FW (g/mol)	692.46	664.44	697.79	703.89	1436.99
Temp. (K)	293	293	293	293	293
$\lambda$ (Å)	0.71073	0.71073	0.71073	0.71073	0.71073
Crystal system	Triclinic	Triclinic	Triclinic	Triclinic	Monoclinic
Space Group	P-1	P-1	P-1	P-1	P21/n
Unit cell					
<i>a</i> (Å)	9.291(1)	9.2708(2)	9.2648(3)	9.2483(14)	10.7422(4)
<i>b</i> (Å)	12.025(2)	11.9699(3)	11.9499(3)	11.9016(15)	17.1435(7)
<i>c</i> (Å)	12.835(2)	12.7725(3)	12.7485(5)	12.6880(19)	14.8397(6)
$\alpha$ (°)	106.491(8)	106.589(1)	106.629(2)	106.599(8)	90
$\beta$ (°)	110.125(9)	110.161(2)	110.177(2)	110.207(7)	93.001(2)
$\gamma$ (°)	99.551(9)	99.377(1)	99.313(2)	99.271(9)	90
Volume (Å <sup>3</sup> )	1234.4(4)	1220.16(6)	1214.98(8)	1202.5(3)	2729.1(2)
Z	2	2	2	2	4
$\rho$ calcd (mg/m <sup>3</sup> )	1.863	1.890	1.907	1.944	1.749
Abs.Coeff (mm <sup>-1</sup> )	1.965	2.234	2.375	2.682	1.777
F(000)	688	692	694	698	1432
$\theta$ range (°)	3.0 to 26.4	3.0 to 26.4	3.0 to 26.4	1.9 to 26.5	3.0 to 26.3
Reflections collected / Unique [R(int)]	9505/4997 [0.049]	37191/4978 [0.136]	38139/4915 [0.134]	14779/4837 [0.021]	5568/5568 [0.1939]
Completeness (%)	98.4	99.8	99.7	97.4	99.7
Data / restraints / parameters	4997/0/358	4978/0/358	4915/0/358	4837/0/358	5568/0/370
Gof on F <sup>2</sup>	0.86	0.97	1.04	1.07	1.03
R1 [ $I > 2\sigma(I)$ ]	0.0384	0.0401	0.0511	0.0222	0.0590
wR2 [ $I > 2\sigma(I)$ ]	0.0831	0.0959	0.1204	0.0529	0.1364

[Ln(3-OHNDSD)(H<sub>2</sub>O)<sub>2</sub>] is a series of isostructural compounds, where Ln = La, Pr, Nd and Sm. They are formed by one metal cation, one molecule of the 3-OHNDSD ligand and two water molecules crystallographically independent. Each metallic center shows an 8-coordinate environment, which forms a distorted square antiprism polyhedron (Fig. 2, a)).<sup>49</sup> Its coordination sphere is formed by four oxygen atoms of the sulfonate group, two oxygen atoms of the phenyl group of the ligand and two coordination water molecules. Sulfonate and phenolate groups join two metallic centers in *syn-syn*  $\mu\eta^2$  and  $\mu\eta^2$  coordination mode, respectively (Fig. 2, b)). This connectivity enabled the formation of shared edge dimers as secondary building units (SBUs) with an intermetallic distance of 4.017(7) Å. SBUs are joined by the remaining sulfonate in *anti-syn*  $\mu\eta^2$  coordination mode and the ligands are arranged alternately for the formation of 2D layers in the plane (011) (Fig. 2, c)) with an interdimeric distance of 5.609(6) Å.

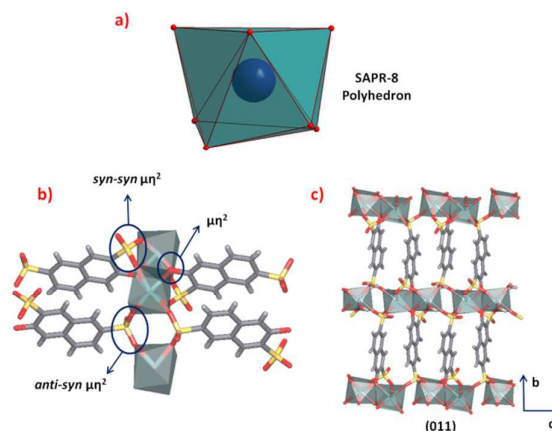


Fig. 2 a) Coordination polyhedra, b) Coordination modes and c) layers in the plane (011) for [Ln(3-OHNDSD)(H<sub>2</sub>O)<sub>2</sub>] compound.

The simplification of 2D network shows SBUs act as a 6-connected node and the ligand joins three dimeric units, giving rise to 3,6-binodal **kgd**; Shubnikov plane (3.6.3.6)/dual net with point symbol  $(4^3)2(4^6.6^6.8^3)$  (Fig. 3).<sup>46</sup>

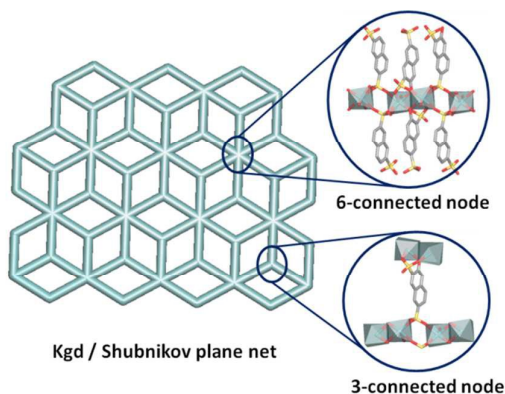


Fig. 3 Topological representation of the 2D network for  $[\text{Ln}(\text{3-OHNSD})(\text{H}_2\text{O})_2]$  compound.

The analysis of the supramolecular structure revealed the coordination water molecules showed strong hydrogen bonds with the oxygen atoms of the sulfonate group with  $\text{O8-H8B}\cdots\text{O2} = 2.712(8)$  and  $\text{O9-H9B}\cdots\text{O5} = 2.821(9)$  Å distances. The stronger hydrogen bonds along the [100] direction make possible to simplify the network and gives it dimensionality. They also give rise to a 3D supramolecular binodal network of *fit-4,8-P42/mmc* type with point symbol  $(4^6)2(4^{12}.6^{10}.8^6)$ . As expected, the product of a new bond between the metallic center and the ligand increased the connectivity of a 6,3-connected nodes to an 8,4-connected nodes network (Fig. 4).<sup>46</sup>

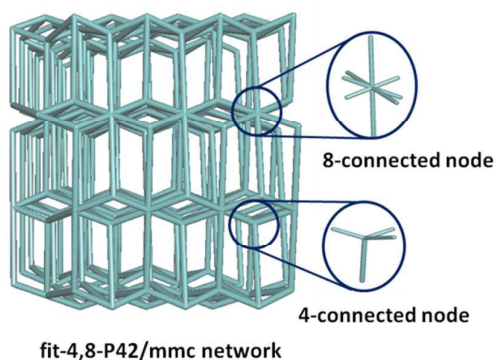


Fig. 4 Topological representation of the 3D supramolecular network for  $[\text{Ln}(\text{3-OHNSD})(\text{H}_2\text{O})_2]$  compound.

$[\text{Ln}(\text{3-OHNSD})(\text{phen})(\text{H}_2\text{O})]\cdot 3\text{H}_2\text{O}$  belongs to a family of compounds, where  $\text{Ln} = \text{La}, \text{Pr}, \text{Nd}$  and  $\text{Sm}$ . The asymmetric unit is comprised of one metallic center, one 3-OHNSD ligand, one molecule of 1,10-phenanthroline, one coordination water molecule and three free water molecules. Each metallic center is bonded to two nitrogen atoms of the phenanthroline molecule, three oxygen atoms of the sulfonate group, two oxygen atoms of the phenyl group and one oxygen atom of the

water molecule, forming an 8-coordinate environment with a distorted square antiprism polyhedron (Fig. 5, a).<sup>49</sup> Two sulfonate groups and two phenolate groups are joined via *syn-syn*  $\mu\eta^2$  and  $\mu\eta^2$  coordination modes, respectively, to two metallic centers. This junction gives rise to dimeric shared edge secondary building units. SBUs are joined by the remaining sulfonate group in  $\eta^1$  coordination mode, which restrains the growth of the polymer to 1D and gives rise to chains along the [010] direction (Fig. 5, b).

The 3D supramolecular packing is given by the hydrogen bonds of water interstitial molecules. Tandem hydrogen bonds formed between  $\text{O8-H8B}\cdots\text{O9-H9B}\cdots\text{O10-H10B}\cdots\text{O6}$  with 2.626(6), 2.799(6) and 2.882(6) Å distances respectively, and  $\text{O8-H8B}\cdots\text{O9-H9B}\cdots\text{O4}$  with an  $\text{O9-H9B}\cdots\text{O4} = 2.972(6)$  Å distance join the polymeric chains along the [100] direction and give rise to a 2D supramolecular arrangement (Fig. 5, c). 3D supramolecular crystal packing is finally formed for weak  $\text{C16-H16}\cdots\text{O4}$  interactions (3.394(9) Å) along the [001] direction.

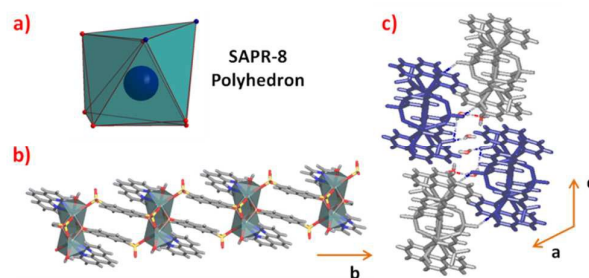
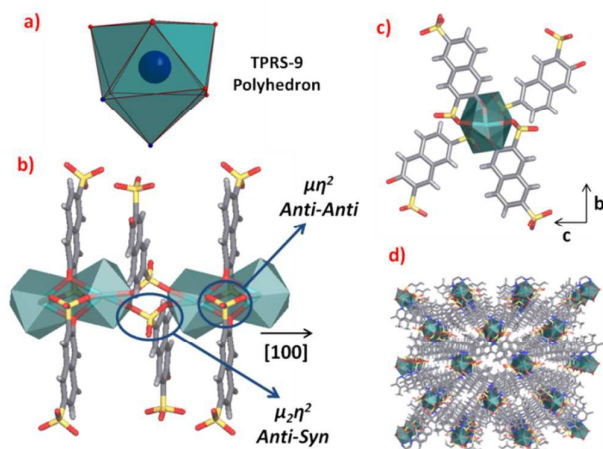


Fig. 5 a) Coordination polyhedra, b) Polymeric chain along the [010] direction and c) crystalline packing and hydrogen bonds for  $[\text{Ln}(\text{3-OHNSD})(\text{phen})(\text{H}_2\text{O})]\cdot 3\text{H}_2\text{O}$  compound.

$[\text{La}(\text{3-OHNSD})(\text{3,4,7,8-TMphen})(\text{H}_2\text{O})]$  compound is formed by one  $\text{La}^{\text{III}}$  metallic center, one 3-OHNSD molecule, one 3,4,7,8-Tetramethyl-1,10-phenanthroline molecule and one coordinated water molecule in its asymmetric unit. The metallic center displays 9-coordinated trigonal prism square face tricapped polyhedron (TPRS-9),<sup>49</sup> comprised of two nitrogen atoms from 3,4,7,8-TMphen, six oxygen atoms of 3-OHNSD and one oxygen atom of the coordinate water molecule. A 3-OHNSD ligand is coordinated to two metallic centers by sulfonate and phenolate groups in *anti-anti*  $\mu_2\eta^2$  and  $\mu\eta^2$  modes, respectively; these coordination modes result in rod-shaped inorganic  $\text{Ln}_2\text{N}_4\text{O}_{10}$  SBUs. On the other hand, the sulfonate group remains and joins SBUs in *anti-syn*  $\mu_2\eta^2$  coordination mode forming inorganic chains along the [100] direction (Fig. 6). The ligand molecules join the inorganic chains in both [011] and [01-1] directions to give rise to a 3D network.

## ARTICLE

## Journal Name



**Fig. 6** a) Coordination polyhedra, b) Representation of the SBUs growing along the [100] direction, c) view of the coordination sphere (3,4,7,8-TMphen ligand has been omitted for clarity) and d) crystal packing along the [100] direction for [La(3-OHNSD)(3,4,7,8-TMphen)(H<sub>2</sub>O)] compound.

The 3D network can be simplified as a binodal 3,6-connected network, where the ligand join three SBUs. The SBUs are linked to six ligand molecules to give rise to **rtl** rutile 3,6-connected topological type with point symbol  $(4.6^2)^2(4^2.6^{10}.8^3)$  (Fig. 7).<sup>46</sup>

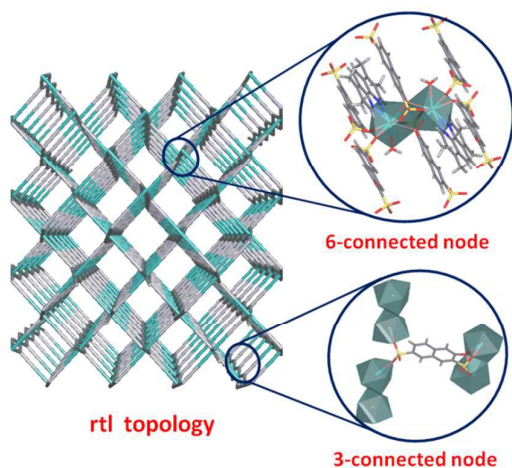


**Fig. 7** Topological representation of the 3D network for [La(3-OHNSD)(3,4,7,8-TMphen)(H<sub>2</sub>O)] compound.

### Structural Analysis.

Several studies have highlighted the weak coordination strength of the sulfonate groups.<sup>50-54</sup> The coordination strength can be changed by the hydrothermal methodology and the use of oxophilic metals as lanthanide metals and some transition metals in the presence of ancillary ligands. This occurs with the

three new families of compounds synthesised under similar hydrothermal reaction conditions, where the presence or absence of an ancillary ligand in the reaction media showed a direct influence in the coordination modes of the 3-OHNSD linker, in the topology and in the crystal packing (Table 2). The 1,10-phenanthroline molecule lock the coordination sphere of the metal limiting their dimensionality. Different situation occurs in presence of the 3,4,7,8-TMphen, where the apolar methyl groups generate apolar voids building the 3D structure. In the case of the [Ln(3-OHNSD)(H<sub>2</sub>O)<sub>2</sub>] compounds, water molecules locked the metal disrupt the network growth.

Table 2. Structural comparison of the Ln-MOFs reported in this work.

Compound	Dimensionality	Topology	Coord. modes
(1)-(4)	2D	kgd, fit	
(5)-(8)	1D	Ladder-shape chains	
(9)	3D	rtl	

A search in the CCDC data base<sup>55</sup> revealed 14 entries of metal-organic compounds, three of them with 3-OHNSD and the others with a similar ligand (2,7-naphthalenedisulfonate). All the entries showed the coordination modes observed in the obtained compounds (Table 2).

As addressed in the structural description of the compounds, these coordination modes generate a particular base for the formation of the whole structure, which is directly related to the functionality and properties. In this case, compounds [Ln(3-OHNSD)(H<sub>2</sub>O)<sub>2</sub>] and [La(3-OHNSD)(3,4,7,8-TMphen)(H<sub>2</sub>O)] exhibit 2D and 3D structures with cavities. In the first case, a void is observed in the inter-laminar space (Fig. 8) and corresponds to approximately 11.5% of the cell volume. In the second case, the 15.8 % of the cell volume are void channels (Fig. 8). The same analysis conducted for 14 CCDC entries revealed only POLHEF<sup>56</sup> compound showed small voids corresponding to 379 Å<sup>3</sup> (12% of the cell volume). These results indicate, in general, the compounds derived from naphthalenedisulfonate display a compact packing arrangement without accessible voids. An exceptional size of the void space is observed for [La(3-OHNSD)(3,4,7,8-TMphen)(H<sub>2</sub>O)] compounds (Fig. 8) in comparison with the 14 entries.

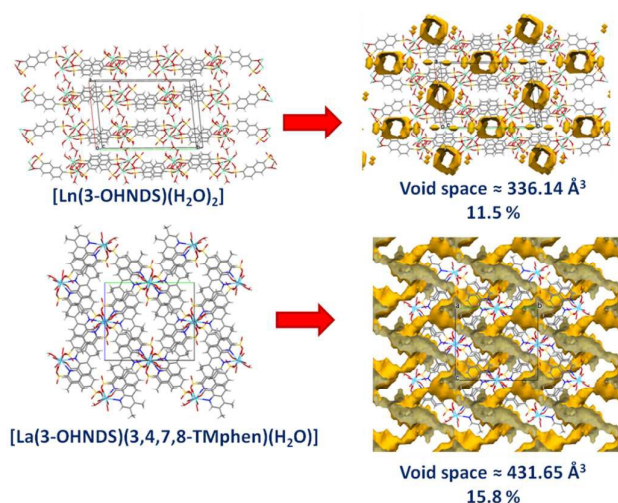


Fig. 8 Solvent accessible surface (Prob. rad.= 0.5, grid=0.7) for  $[\text{Ln}(3\text{-OHNDS})(\text{H}_2\text{O})_2]$  and  $[\text{La}(3\text{-OHNDS})(3,4,7,8\text{-TMphen})(\text{H}_2\text{O})]$  compounds (Crystal voids calculation: Mercury)

### Thermal study.

$[\text{Ln}(3\text{-OHNDS})(\text{H}_2\text{O})_2]$  compounds show a similar thermal profile with a mass loss around  $\sim 180\text{-}190 \text{ }^\circ\text{C}$ , which corresponds to the loss of two coordinated water molecules (mass loss calculated: 7.5%, observed: 6.51%). The total decomposition is observed at around  $\sim 420 \text{ }^\circ\text{C}$ .  $[\text{Ln}(3\text{-OHNDS})(\text{phen})(\text{H}_2\text{O})] \cdot 3 \text{ H}_2\text{O}$  compounds showed a mass loss around  $\sim 50 \text{ }^\circ\text{C}$  of three physisorbed water molecules (mass loss calculated: 7.73%, observed: 6.96%), followed by a total decomposition at  $\sim 480 \text{ }^\circ\text{C}$ . Finally,  $[\text{La}(3\text{-OHNDS})(3,4,7,8\text{-TMphen})(\text{H}_2\text{O})]$  compound showed a mass loss corresponding to a coordinated water molecule at  $\sim 120 \text{ }^\circ\text{C}$  (mass loss calculated: 2.59%, observed: 2.96%) and decomposition at  $410 \text{ }^\circ\text{C}$  (Supp. Inf. S2). All the compounds obtained showed high thermal stability up to  $400 \text{ }^\circ\text{C}$ .

### IR Analysis.

The IR spectra for the  $[\text{Ln}(3\text{-OHNDS})(\text{H}_2\text{O})_2]$  and  $[\text{Ln}(3\text{-OHNDS})(\text{phen})(\text{H}_2\text{O})] \cdot 3 \text{ H}_2\text{O}$  series showed the same profile for each family of compounds (Supp. Inf. S3). C-H vibrations belonging to aromatic rings of the 3-OHNDS and phenanthroline ligands are found at around  $\sim 3060 \text{ cm}^{-1}$  for both compounds. The bands located at approximately  $\sim 3370 \text{ cm}^{-1}$  are assigned to the O-H vibration of the water molecules coordinated for  $[\text{Ln}(3\text{-OHNDS})(\text{H}_2\text{O})_2]$  compound. The same vibrations for coordinated and free water molecules are observed around  $\sim 3550\text{-}3370 \text{ cm}^{-1}$  in  $[\text{Ln}(3\text{-OHNDS})(\text{phen})(\text{H}_2\text{O})] \cdot 3 \text{ H}_2\text{O}$  compounds. The intense band present at around  $\sim 1050\text{-}1030 \text{ cm}^{-1}$  is assigned to the C-O vibration of the phenolate group. S=O and S-O vibrations observed in the  $\sim 1240\text{-}1100 \text{ cm}^{-1}$  region are related to the coordination of the sulfonate group. In this region, four bands characteristic of the bridged bidentate complex ( $\mu_1^2$ ) are also found. The peaks around  $\sim 520\text{-}340 \text{ cm}^{-1}$  are assigned to the

different M-O and M-N vibrations modes present in the compounds.<sup>57</sup>

$[\text{La}(3\text{-OHNDS})(3,4,7,8\text{-TMphen})(\text{H}_2\text{O})]$  MOF showed methyl and aryl C-H vibration around  $\sim 3150\text{-}2850 \text{ cm}^{-1}$ . The bands around  $\sim 3660\text{-}3200 \text{ cm}^{-1}$  are assigned to the O-H vibration of the coordinated water molecules. The band located at  $1035 \text{ cm}^{-1}$  belongs to the C-O vibration of the phenolate group. Bands corresponding to the S=O and S-O vibration modes of the sulfonate group are found at  $\sim 1220\text{-}1100 \text{ cm}^{-1}$ . Finally, the peaks found around  $\sim 515\text{-}340 \text{ cm}^{-1}$  correspond to the M-O and M-N vibrations (Supp. Inf. S3).

### Optical properties.

Lanthanide ions are excellent candidates as luminescent centers for applications, such as scintillating, lighting, thermometry, sensors and optoelectronic devices.<sup>22</sup> One of the optical characteristics of trivalent lanthanide ions are  $4f\text{-}4f$  transitions, which show sharp lines in their emission spectra. After coordination, the organic ligands can transfer their energy absorbed from light radiation to lanthanide ions (*Antenna Effect*). This process is commonly seen in compounds that incorporate chromophores either as ligands, or as guest molecules that act as antennas for light absorption. The PL properties of compounds (1)-(8) are reported in comparison with the 3-OHNDS ligand. As shown in Fig. 9, the 3-OHNDS ligand exhibits a blue fluorescent emission characterized by bands located at  $379.1 (26378 \text{ cm}^{-1})$  and  $415.9 \text{ nm} (24044 \text{ cm}^{-1})$  after excitation with  $\lambda_{\text{exc}}=308 \text{ nm} (32468 \text{ cm}^{-1})$ , attributable to the typical  $\pi^* \rightarrow \pi$  or  $\pi^* \rightarrow n$  transitions of aromatic ligands.<sup>58</sup> To the best of our knowledge, this is the first time where PL properties of the 3-OHNDS are explored. The assignment of the observed electronic transitions in the excitation-emission 3-OHNDS spectra (labels a-d) is shown in Table S1 (Supp. Inf. S5).

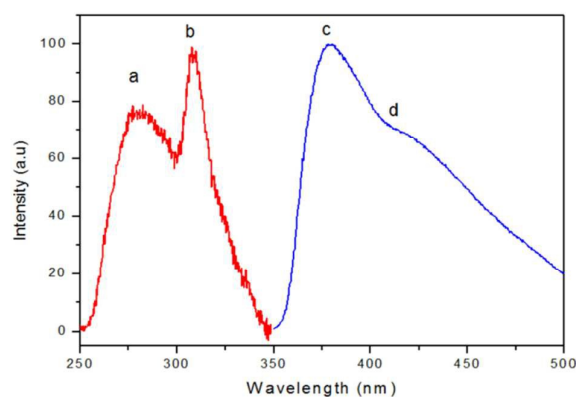


Fig. 9 Excitation to  $\lambda_{\text{exc}}=308 \text{ nm}$  (red) and emission (blue) spectra of 3-OHNDS.

Compounds (1) and (5) contain non-emissive  $\text{La}^{\text{III}}$  ions, which exhibit broad intense emission bands centered at  $431.9 (23154 \text{ cm}^{-1})$  and  $430.2 \text{ nm} (23245 \text{ cm}^{-1})$  upon excitation at 308 (for 1) and 306 (for 5) nm, respectively. The emission are assigned to intra-ligand  $n \rightarrow \pi^*$  or  $\pi \rightarrow \pi^*$  transitions from the organic moieties. In both cases a considerable red-shift is observed with respect to the ligand emission ( $51.1 \text{ nm}$  for 1 and  $52.8 \text{ nm}$

## ARTICLE

## Journal Name

for 5). According to the spectra exhibited for the La<sup>III</sup> compounds, the emissions are more intense than that of the free ligand (see Fig. 10), which could be justified in terms of the *rigidity* produced by aromatic linkers.<sup>59</sup> The rigidity of the coordinated ligand reduces the loss of energy by non-radiative processes increasing the emission efficiency.<sup>60, 61</sup> The presence of phenanthroline as an ancillary ligand directly coordinated to the metal centers in (5) produces more stiffness in the compound than that presented in (1), which is coordinated only by 3-OHNDS and water ligands. This structural difference enables enhance luminescence over the free ligand 3-OHNDS (16 % for 1 and 184% for 5). Besides, the calculated lifetimes values found for (1) and (5) were 16 and 17.5 ns, whose difference could be explained for the same mentioned process. The corresponding luminescence decay traces for both compounds can be seen in Supp. Inf. S6. To present the nature of the emitted light from 3-OHNDS, (1) and (5) under the corresponding excitation wavelength, a CIE chromaticity diagram is displayed in Fig. 14. As can be seen, the La compounds emit blue radiation.

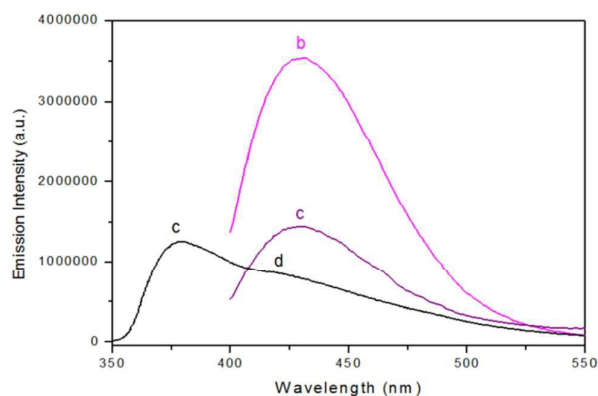


Fig. 10 Emission spectra of 1 (purple) and 5 (pink) in comparison with the spectrum of 3-OHNDS free ligand.

The excitation spectra of the two studied Pr-based compounds (2 and 6) exhibit similar intense broad bands with  $\lambda_{\text{max}}$  located at 394.9 (25323 cm<sup>-1</sup>) (2) and 413.6 nm (24178 cm<sup>-1</sup>) (6), respectively, related to  $n \rightarrow \pi^*$  or  $\pi \rightarrow \pi^*$  transitions from aromatic groups. Lower intensity peaks corresponding to transitions within the Pr<sup>III</sup> ion's 4f shell (see Fig. S4.3 and S4.4) can be identified in the spectra. Therefore, those wavelengths had been selected as excitation during the recording of the emission spectra. The higher intensity of the band in both compounds indicates an effective *antenna effect*. The corresponding emission spectra are shown in Fig. 11. Table S1 (Supp. Inf. S5) displays transitions corresponding to the labeled peaks. Both emission spectra show red-shifted ligand-centered  $\pi^* \rightarrow \pi$  (or  $\pi^* \rightarrow n$ ) transitions (449.1, 466, 529.1 nm in (2); and 451.9, 463.8 and 525.9 nm for (6)) compared with the 3-OHNDS free ligand. The red-shift (87 and 85 nm, (2) and (6) respectively) is attributed to metal-disturbed ligand-centered transitions.<sup>62</sup> Moreover, characteristic Pr<sup>III</sup> bands assignable to the radiative decay from <sup>3</sup>P<sub>0</sub> and <sup>1</sup>D<sub>2</sub> levels (see assignments in Table S1) could be identified. An important difference between

the spectra is a major contribution of aromatic transitions in (6) than in (2) justified by the presence of phenanthroline as an ancillary ligand. These facts make compounds (2) and (6) emitting greenish blue and bluish green lights respectively (see Fig. 14). Monitoring the luminescence decay of the <sup>3</sup>P<sub>0</sub> → <sup>3</sup>H<sub>4</sub> transition of both compounds, the curves could be fitted by biexponential functions (see Supp. Inf. S6). The calculated lifetimes were 4.7 and 8.9 ns for (2) and (6) respectively.

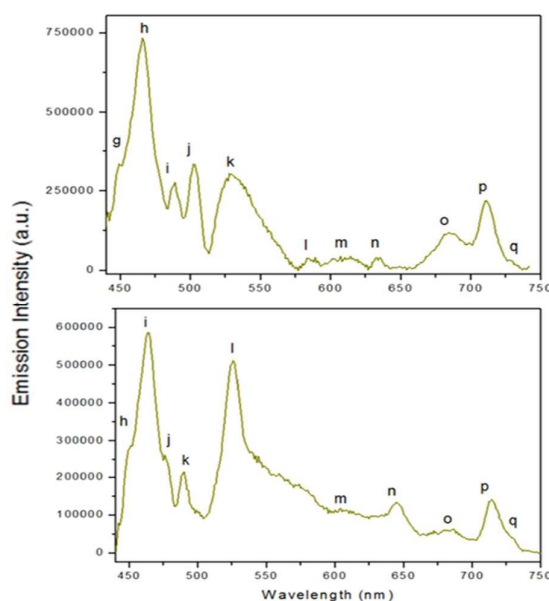


Fig. 11 Emission spectra of 2 (left) and 6 (right). The labels correspond to the electronic transitions shown in Table S1 (Supp. Inf. S5).

The excitation spectra of the Nd<sup>III</sup>-based compounds are composed of broad bands originated by  $\pi^* \leftarrow n$  or  $\pi^* \leftarrow \pi$  transitions from the ligands (see Fig. S4.5 and S4.6). Upon excitation at 280 (35714 cm<sup>-1</sup>) and 345.9 (28910 cm<sup>-1</sup>) nm, both compounds exhibit blue-green luminescence. As in compounds (2) and (6), (3) and (7) show ligand sensitization. So the emission spectra show a ligand-centered emission characterized by  $\pi^* \rightarrow \pi$  (or  $\pi^* \rightarrow n$ ) transitions accompanied by bands related to Nd<sup>III</sup> ion's 4f shell transitions. Fig. 12 shows the spectra with the emission transitions labels for the compounds and the corresponding assignments are displayed in Table S1 (Supp. Inf. S5). Despite the huge information related to up-conversion processes in Nd-MOFs,<sup>8c</sup> the report of PL properties in the visible region is scarce. Here we report the 4f-4f rarely reported transitions in the visible region belonging to <sup>2</sup>P<sub>3/2</sub> → <sup>4</sup>I<sub>9/2</sub>, <sup>2</sup>P<sub>3/2</sub> → <sup>4</sup>I<sub>11/2</sub> and <sup>2</sup>G<sub>7/2</sub> + <sup>4</sup>G<sub>5/2</sub> → <sup>4</sup>I<sub>9/2</sub> transitions, which have been identified only in neodymium doped inorganic matrixes, such as aluminates, fluorides and tungstates.<sup>63-65</sup> As seen in the emission spectra of (3) and (7), the ligand-centered emissions are similar in intensities, however the <sup>2</sup>G<sub>7/2</sub> + <sup>4</sup>G<sub>5/2</sub> → <sup>4</sup>I<sub>9/2</sub> transition is more intense in (3)

than in (7). This observation can be justified by the water content in both structures: in compound (7), the interstitial water molecules that reinforce the supramolecular structure combined with the presence of one coordinated water molecule contribute to a *multiphonon relaxation*. This mechanism explains non-radiative deactivations in systems containing rare earths as emissive centers.<sup>23, 66</sup> However, this fact seems not affect the lifetime values obtained after monitoring the emission decay of the  ${}^2G_{7/2}+{}^4G_{5/2}\rightarrow{}^4I_{9/2}$  4f transition (560 nm), being 0.293 and 0.308  $\mu\text{s}$  for (3) and (7). The corresponding decay traces with biexponential fittings are displayed in Supp. Inf. S6.

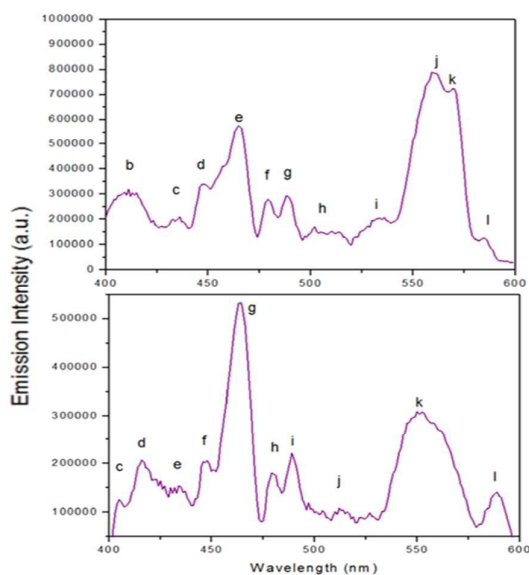


Fig. 12 Emission spectra of 3 (up) and 7 (down).

As shown in Fig. S4.7 and S4.8, the excitation spectra of compounds (4) and (8) consist in intense broad bands (labeled a-b) associated with  $\pi^*\leftarrow\pi$  or  $\pi^*\leftarrow n$  transitions, followed by lines corresponding to transitions within the  $\text{Sm}^{\text{III}}$  ion's 4f shell. The emission spectra of both compounds were obtained under excitation wavelengths of 380.6 (4) ( $26274\text{ cm}^{-1}$ ) and 382.6 (8) nm ( $26137\text{ cm}^{-1}$ ) (see Fig. 13). The spectra contain the typical transitions of  $\text{Sm}^{\text{III}}$  corresponding to the decay radiative process from the  ${}^4G_{5/2}$  to  ${}^6H_{5/2}$ ,  ${}^6H_{7/3}$ ,  ${}^6H_{9/4}$  and  ${}^6H_{11/2}$  levels. The assigned transitions are shown in Table S1 (Supp. Inf. S5).

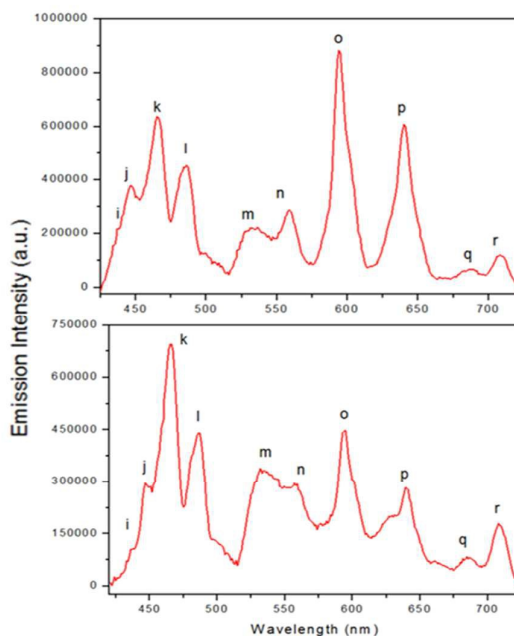


Fig. 13 Emission spectra of 4 (up) and 8 (down).

The Sm-compounds exhibit ligand-centered  $\pi^*\rightarrow\pi$  (or  $\pi^*\rightarrow n$ ) transitions with  $\lambda_{\text{max}}$  located at 483.7 ( $20674\text{ cm}^{-1}$ ) and 486.4 nm ( $20559\text{ cm}^{-1}$ ) for (4) and (8) respectively. These transitions are red-shifted compared with the free 3-OHNSD ligand (104.6 and 86.3 nm). The 4f-4f transitions in (4) are more intense than the bands from the ligand emission. In contrast with the previous scenario, the lanthanide related bands in compound (8) are less intense than the ligand-centered transitions. Through monitoring the luminescence decay of the labeled "o" ( ${}^4G_{5/2}\rightarrow{}^6H_{7/3}$ ) transition was possible obtain significantly different lifetimes (4.72 (4) and 41 ns for (8)). These observations can be related with the water content in both structures that efficiently quench the lanthanide luminescence in (8). Therefore, this changes the impression of the emission color from a purplish pink in compound (4) to practically white in (8) (x,y coordinates 0.31, 0.32) (see Fig. 14). The Sm-compounds exhibit ligand-centered  $\pi^*\rightarrow\pi$  (or  $\pi^*\rightarrow n$ ) transitions with  $\lambda_{\text{max}}$  located at 483.7 ( $20674\text{ cm}^{-1}$ ) and 486.4 nm ( $20559\text{ cm}^{-1}$ ) for (4) and (8) respectively. These transitions are red-shifted compared with the free 3-OHNSD ligand (104.6 and 86.3 nm). The 4f-4f transitions in (4) are more intense than the bands from the ligand emission. In contrast with the previous scenario, the lanthanide related bands in compound (8) are less intense than the ligand-centered transitions. Through monitoring the luminescence decay of the labeled "o" ( ${}^4G_{5/2}\rightarrow{}^6H_{7/3}$ ) transition was possible obtain significantly different lifetimes (4.72 (4) and 41 ns for (8)). These observations can be related with the water content in both structures that efficiently quench the lanthanide luminescence in (8). Therefore, this changes the impression of the emission color from a purplish pink in compound (4) to practically white in (8) (x,y coordinates 0.31, 0.32) (see Fig. 14). White-light-emitting materials (x,y coordinates for white light emitters

## ARTICLE

## Journal Name

0.33, 0.33) and devices have attracted interest because of their potential applications to solid-state lighting (SSL), full-color displays and backlights.<sup>67-69</sup> To date, most white-light sources depend on the combination of the emissions from separate dopants, which may cause problems, such as phase separation and color variation. In order to avoid these inconvenients the fact of obtain materials made of single-phosphor giving rise white-light, is an important target.

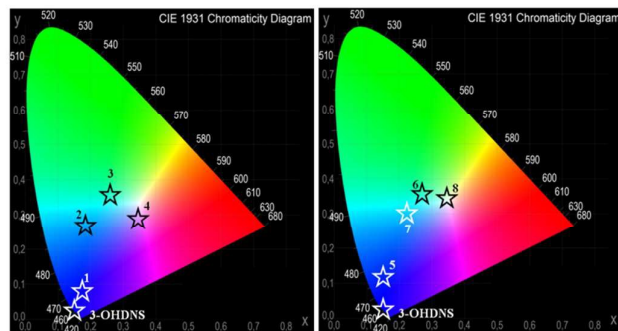


Fig. 14 CIE diagram for compounds 1-8. The corresponding x,y coordinates are displayed in Table S2 (Supp. Inf. S6).

## Conclusions

Nine new compounds grouped into three families from 3-Hydroxinaftalene-2,7-disulfonic acid, lanthanide metals and two different phenanthroline ancillary ligands were obtained. The new crystalline compounds form 1D, 2D and 3D networks, depending on the ancillary ligand. [La(3-OHNDNS)(3,4,7,8-TMphen)(H<sub>2</sub>O)] is the first lanthanide-based compound with a 3D network and rti topology obtained with the 3,4,7,8-TMphen as an ancillary ligand, in agreement to the search in the CCDC data base. Moreover, the PL properties of all 1D and 2D compounds were explored in terms of excitation-emission spectra, x,y CIE chromaticities and lifetime values. The photoluminescence of the 3-OHNDNS ligand was explored and compared with those of the lanthanide compounds. The emission spectra were obtained by direct excitation from the energy levels of the ligand, which confirms *antenna effect* or ligand sensitization of the 3-OHNDNS ligand. These studies demonstrated that both ligand and lanthanide-centered emissions are presented in the two sets of compounds. Their PL features are strongly affected by two structural aspects: firstly, the presence of ancillary ligands such as phenanthroline which confers *molecular rigidity*, and secondly the existence of water molecules of coordination and hydration which can efficiently quench the lanthanide emissions. The strategy that involves the use of ancillary ligands seems to be a promising method for the obtaining lanthanide based compounds with different dimensionalities. Moreover, this approach could be considered as an interesting way of preparation materials with potential optical applications.

## Acknowledgements

R. D. Acknowledges Coordenação de Aperfeiçoamento de Pessoal de Nível Superior for the CAPES/PNPD scholarship from the Brazilian Ministry of Education, to M. Soto-Monsalve for measures and FAPESP (2009/54011-8) for provide Apex-II equipment. J.E. is grateful to CNPq for the research fellowships. G. E. G. acknowledges a postdoctoral CONICET (Consejo Nacional de Investigaciones Científicas y Técnicas) fellowship.

## References

1. N. Stock and S. Biswas, *Chem. Rev.*, 2012, **112**, 933-969.
2. R. F. D'Vries, M. Iglesias, N. Snejko, S. Alvarez-Garcia, E. Gutierrez-Puebla and M. A. Monge, *J. Mater. Chem.*, 2012, **22**, 1191-1198.
3. R. F. D'Vries, I. Camps and J. Ellena, *Cryst. Growth Des.*, 2015, **15**, 3015-3023.
4. G. E. Gomez, M. C. Bernini, E. V. Brusau, G. E. Narda, W. A. Massad and A. Labrador, *Cryst. Growth Des.*, 2013, **13**, 5249-5260.
5. M. Clemente-Leon, E. Coronado, C. Marti-Gastaldo and F. M. Romero, *Chem. Soc. Rev.*, 2011, **40**, 473-497.
6. D. J. Tranchemontagne, K. S. Park, H. Furukawa, J. Eckert, C. B. Knobler and O. M. Yaghi, *J. Phys. Chem. C*, 2012, **116**, 13143-13151.
7. H. Furukawa, K. E. Cordova, M. O'Keeffe and O. M. Yaghi, *Science*, 2013, **341**.
8. H. Furukawa, U. Müller and O. M. Yaghi, *Angew. Chem. Int. Ed.*, 2015, 3417-3430.
9. P. Peng, F.-F. Li, V. S. P. K. Neti, A. J. Metta-Magana and L. Echegoyen, *Angew. Chem. Int. Ed.*, 2014, **53**, 160-163.
10. P. A. Sontz, J. B. Bailey, S. Ahn and F. A. Tezcan, *J. Am. Chem. Soc.*, 2015, **137**, 11598-11601.
11. O. K. Farha, I. Eryazici, N. C. Jeong, B. G. Hauser, C. E. Wilmer, A. A. Sarjeant, R. Q. Snurr, S. T. Nguyen, A. Ö. Yazaydin and J. T. Hupp, *J. Am. Chem. Soc.*, 2012, **134**, 15016-15021.
12. Y. Peng, V. Krungleviciute, I. Eryazici, J. T. Hupp, O. K. Farha and T. Yildirim, *J. Am. Chem. Soc.*, 2013, **135**, 11887-11894.
13. L. Du, Z. Lu, K. Zheng, J. Wang, X. Zheng, Y. Pan, X. You and J. Bai, *J. Am. Chem. Soc.*, 2013, **135**, 562-565.
14. J. F. M. Denayer., D. D. Vos. and P. Leflaive, in *Metal-Organic Frameworks: Applications from Catalysis to Gas Storage* ed. D. Farrusseng, Wiley-VCH., 2011, pp. 173-187.
15. M. Zhang, G. Feng, Z. Song, Y.-P. Zhou, H.-Y. Chao, D. Yuan, T. Y. Tan, Z. Guo, Z. Hu, B. Z. Tang, B. Liu and D. Zhao, *J. Am. Chem. Soc.*, 2014, **136**, 7241-7244.
16. W. Wang, J. Yang, R. Wang, L. Zhang, J. Yu and D. Sun, *Cryst. Growth Des.*, 2015, **15**, 2589-2592.
17. J. Della Rocca, D. Liu and W. Lin, *Acc. Chem. Res.*, 2011, **44**, 957-968.
18. Z. Ma and B. Moulton, *Coord. Chem. Rev.*, 2011, **255**, 1623-1641.
19. R. F. D'Vries, M. Iglesias, N. Snejko, E. Gutiérrez-Puebla and M. A. Monge, *Inorg. Chem.*, 2012, **51**, 11349-11355.

20. J. Lee, O. K. Farha, J. Roberts, K. A. Scheidt, S. T. Nguyen and J. T. Hupp, *Chem. Soc. Rev.*, 2009, **38**, 1450-1459.
21. J. Gascon, A. Corma, F. Kapteijn and F. X. Llabrés i Xamena, *ACS Catalysis*, 2014, **4**, 361-378.
22. R. F. D'Vries, S. Alvarez-Garcia, N. Snejko, L. E. Bausa, E. Gutierrez-Puebla, A. de Andres and M. A. Monge, *J. Mater. Chem. C*, 2013, **1**, 6316-6324.
23. G. E. Gomez, M. C. Bernini, E. V. Brusau, G. E. Narda, D. Vega, A. M. Kaczmarek, R. Van Deun and M. Nazzarro, *Dalton Trans.*, 2015, **44**, 3417-3429.
24. M. D. Allendorf, C. A. Bauer, R. K. Bhakta and R. J. T. Houk, *Chem. Soc. Rev.*, 2009, **38**, 1330-1352.
25. J.-C. G. Bünzli, S. Comby, A.-S. Chauvin and C. D. B. Vandevyver, *J. Rare Earths*, 2007, **25**, 257-274.
26. E. Coronado and G. Minguez Espallargas, *Chem. Soc. Rev.*, 2013, **42**, 1525-1539.
27. Q.-G. Zhai, C. Mao, X. Zhao, Q. Lin, F. Bu, X. Chen, X. Bu and P. Feng, *Angew. Chem. Int. Ed.*, 2015, **54**, 7886-7890.
28. S. Kim, K. W. Dawson, B. S. Gelfand, J. M. Taylor and G. K. H. Shimizu, *J. Am. Chem. Soc.*, 2013, **135**, 963-966.
29. Y. Cui, Y. Yue, G. Qian and B. Chen, *Chem. Rev.*, 2011, **112**, 1126-1162.
30. D. T. de Lill, N. S. Gunning and C. L. Cahill, *Inorg. Chem.*, 2005, **44**, 258-266.
31. W. Lu, Z. Wei, Z.-Y. Gu, T.-F. Liu, J. Park, J. Park, J. Tian, M. Zhang, Q. Zhang, T. Gentle lli, M. Bosch and H.-C. Zhou, *Chem. Soc. Rev.*, 2014, **43**, 5561-5593.
32. F. Gándara, A. García-Cortés, C. Cascales, B. Gómez-Lor, E. Gutiérrez-Puebla, M. Iglesias, A. Monge and N. Snejko, *Inorg. Chem.*, 2007, **46**, 3475-3484.
33. W.-P. Xie, N. Wang, Y. Long, X.-R. Ran, J.-Y. Gao, C.-J. Chen, S.-T. Yue and Y.-P. Cai, *Inorg. Chem. Commun.*, 2014, **40**, 151-156.
34. J. Perles, N. Snejko, M. Iglesias and M. A. Monge, *J. Mater. Chem.*, 2009, **19**, 6504-6511.
35. J.-P. Zhao, B.-W. Hu, F.-C. Liu, X. Hu, Y.-F. Zeng and X.-H. Bu, *CrystEngComm*, 2007, **9**, 902-906.
36. A. P. Côté and G. K. H. Shimizu, *Coord. Chem. Rev.*, 2003, **245**, 49-64.
37. G. K. H. Shimizu, R. Vaidyanathan and J. M. Taylor, *Chem. Soc. Rev.*, 2009, **38**, 1430-1449.
38. S. Zhang, Y. Yang, Z.-Q. Xia, X.-Y. Liu, Q. Yang, Q. Wei, G. Xie, S.-P. Chen and S.-L. Gao, *Inorg. Chem.*, 2014, **53**, 10952-10963.
39. Z. Otwinowski and W. Minor, *Methods in Enzymology*, Academic Press, New York, 1997.
40. I. Bruker-AXS, *Journal*, 2006.
41. I. Bruker-Siemens, *Journal*, 1997.
42. G. Sheldrick, *Acta Crystallogr. A*, 2008, **64**, 112-122.
43. L. Farrugia, *J. Appl. Crystallogr.*, 2012, **45**, 849-854.
44. O. V. Dolomanov, L. J. Bourhis, R. J. Gildea, J. A. K. Howard and H. Puschmann, *J. Appl. Crystallogr.*, 2009, **42**, 339-341.
45. K. Brandenburg, H. Putz, Diamond, Crystal Impact: Bonn, Germany, 2006.
46. V. A. Blatov, A. P. Shevchenko and D. M. Proserpio, *Cryst. Growth Des.*, 2014, **14**, 3576-3586.
47. C. F. Macrae, I. J. Bruno, J. A. Chisholm, P. R. Edgington, P. McCabe, E. Pidcock, L. Rodriguez-Monge, R. Taylor, J. Van De Streek and P. A. Wood, *J. Appl. Crystallogr.*, 2008, **41**, 466-470.
48. A. Spek, *Acta Crystallogr. D*, 2009, **65**, 148-155.
49. N. G. Connelly, ; Damhus, T.;Hartshorn, R.M.; Hutton, A.T., *Nomenclature of Inorganic Chemistry - IUPAC Recommendations 2005*, RSC Publishing, Cambridge, UK., 2005.
50. J. Cai, *Coord. Chem. Rev.*, 2004, **248**, 1061-1083.
51. J. Cai, C.-H. Chen, C.-Z. Liao, J.-H. Yao, X.-P. Hu and X.-M. Chen, *J. Chem. Soc., Dalton Trans.*, 2001, 1137-1142.
52. R. F. D'Vries, N. Snejko, E. Gutiérrez-Puebla, M. Iglesias and M. Angeles Monge, *Inorg. Chim. Acta*, 2012, **382**, 119-126.
53. A. Monge, F. Gandara, E. Gutierrez-Puebla and N. Snejko, *CrystEngComm*, 2011, **13**, 5031-5044.
54. V. Videnova-Adrabska, *Coord. Chem. Rev.*, 2007, **251**, 1987-2016.
55. F. Allen, *Acta Crystallogr. B*, 2002, **58**, 380-388.
56. Y.-M. Chen and Q.-F. Xie, *Chin. J. Inorg. Chem.*, 2014, **30**, 517.
57. K. Nakamoto, ed., *Infrared and Raman Spectra of Inorganic and Coordination Compounds*, JOHN WILEY & SONS, INC., Hoboken, New Jersey, 2009.
58. W. Chen, J.-Y. Wang, C. Chen, Q. Yue, H.-M. Yuan, J.-S. Chen and S.-N. Wang, *Inorg. Chem.*, 2003, **42**, 944-946.
59. A. J. Lees, *Comments Inorg. Chem.*, 1995, **17**, 319-346.
60. A. Rodriguez-Dieguez, A. Salinas-Castillo, A. Sironi, J. M. Seco and E. Colacio, *CrystEngComm*, 2010, **12**, 1876-1879.
61. C. A. Bauer, S. C. Jones, T. L. Kinnibrugh, P. Tongwa, R. A. Farrell, A. Vakil, T. V. Timofeeva, V. N. Khrustalev and M. D. Allendorf, *Dalton Trans.*, 2014, **43**, 2925-2935.
62. P. Wang, R.-Q. Fan, Y.-L. Yang, X.-R. Liu, P. Xiao, X.-Y. Li, W. Hasi and W.-W. Cao, *CrystEngComm*, 2013, **15**, 4489-4506.
63. J. Martincik, S. Ishizu, K. Fukuda, T. Suyama, T. Cechak, A. Beitlerova, A. Yoshikawa and M. Nikl, *Opt. Mater.*, 2012, **34**, 1029-1033.
64. M. Guzik, J. Cybińska, E. Tomaszewicz, Y. Guyot, J. Legendziewicz, G. Boulon and W. Stręk, *Opt. Mater.*, 2011, **34**, 487-495.
65. V. V. Osipov, V. I. Solomonov and A. V. Spirina, *J. Opt. Technol.*, 2011, **78**, 408-412.
66. G.-F. Hou, H.-X. Li, W.-Z. Li, P.-F. Yan, X.-H. Su and G.-M. Li, *Cryst. Growth Des.*, 2013, **13**, 3374-3380.
67. B. W. D'Andrade and S. R. Forrest, *Adv. Mater.*, 2004, **16**, 1585-1595.
68. Y. H. Niu, M. S. Liu, J. W. Ka, J. Bardeker, M. T. Zin, R. Schofield, Y. Chi and A. K. Y. Jen, *Adv. Mater.*, 2007, **19**, 300-304.
69. H.-C. Su, H.-F. Chen, F.-C. Fang, C.-C. Liu, C.-C. Wu, K.-T. Wong, Y.-H. Liu and S.-M. Peng, *J. Am. Chem. Soc.*, 2008, **130**, 3413-3419.

## Graphical Abstract

**Tuning the Structure, dimensionality and Luminescent properties of Lanthanide Metal-Organic Frameworks under Ancillary Ligand Influence. †**Richard F. D'Vries,<sup>a\*</sup> German E. Gomez,<sup>b</sup> José H. Hodak,<sup>c</sup> Galo J. A. A. Soler-Illia,<sup>b</sup> Javier Ellena.<sup>a</sup>*Dalton Trans.* **2015,**

This manuscript addresses the synthesis, structural characterization and optical properties of a 1D coordination polymer (CPs) and 2D and 3D Metal-Organic Frameworks (MOFs) obtained from lanthanide metals, 3-Hydroxinaftalene-2,7-disulfonic acid (3-OHNSD) and two different phenanthroline derivatives as ancillary ligands.

